Finite Element Analysis of I.C. Engine Piston –Ring

Shubham Bhawsar[1], Prof K.K. Jain[2]
[1] *Research Scholar, department of mechanical Eng. SRIT, Jabalpur (M.P)*
[2]*Professor, department of mechanical Eng. SRIT, Jabalpur (M.P)*

***Abstract*- Piston rings have been being used for whatever length of time that ignition motors themselves. Regardless of this, obliviousness or lacking information of piston rings is still every now and again clear today. No other segment is so basic when control misfortune and oil utilization are in question. With no other part in the motor is the partition amongst desires and used capital more noteworthy than when supplanting piston rings. Very regularly, trust in piston rings endures because of the misrepresented requests made on them. As demonstrated in before, basic outlines of piston rings are not examined sufficiently. Henceforth, the extent of this venture includes following goals:To carry out the Finite Element Analysis of piston rings subjected to various loads acting on it. With also ,Compare the three different material i.e. Grey Cast Iron, Aluminium Alloy and Carbide Malleable Iron for Piston Ring using Finite Element Analysis.**

***Index Terms*- Piston, Piston-Ring, ANSYS, Rectangular Cross Section and Tapered Face Cross Section piston rings**

I. INTRODUCTION

The first need for minimizing the fluid leakage between the piston and the cylinder bore occurred in many types of machinery, water pumps, combustion engines, air compressors, hydraulic motors, hydraulic pumps and others. In the early steam engines no piston rings were used. The temperatures and the steam pressures were not so high. Increasing power demands required higher temperatures, which caused stronger heat expansion of the piston material. Initial attempt to make an extremely narrow gap resulted in very low efficiency. The solution was found in isolating the sealing function and making a separate element – the piston ring – that could better conform to the contact surface of the cylinder bore or cylinder liner. The very first piston ring was made of rope and assembled into a steam engine in 1774 – thermal efficiency increased to 1.4 %. It had the sole task of sealing off the combustion chamber, thus preventing the combustion gases from trailing down into the crankcase. This development increased the effective pressure on the piston.

A piston ring is a split ring used in internal combustion engines to fulfill three main functions:

- seal the combustion chamber from transferring gasses into the crankcase,
- assure the heat flow from the piston to the cylinder andprevent the oil, not required for grease, from going from the crankcase to the burning chamber and to give a uniform oil film on the barrel bore surface.

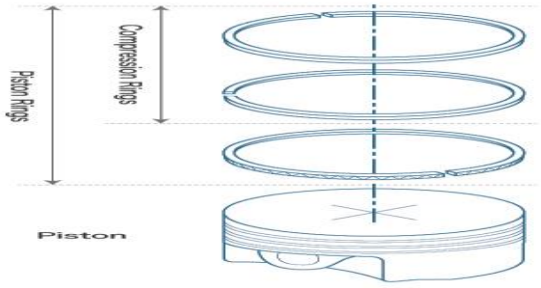

Figure 1.1 Typical ring pack for Internal Combustion Engine

1.1 Piston Ring Design

Piston rings are metallic seals which have the capacity of fixing the ignition chamber from the crankcase and assuring the stream of warmth from the piston to the barrel. Different capacities are to keep the oil not required for grease from going from the crankcase to the burning chamber and to give a uniform oil film on the barrel bore surface. Piston rings are categorized into three basic types:

- compression rings,
- scraper rings and
- oil control rings.

The piston rings form a ring pack, which usually consists of 2-5 rings, including at least one compression ring. The quantity of rings in the ring pack relies upon the motor sort, however for the most

part includes 2-4 pressure rings and 0-3 oil control rings (two-stroke start touched off motors don't have an oil control ring since they have grease blended in the fuel).

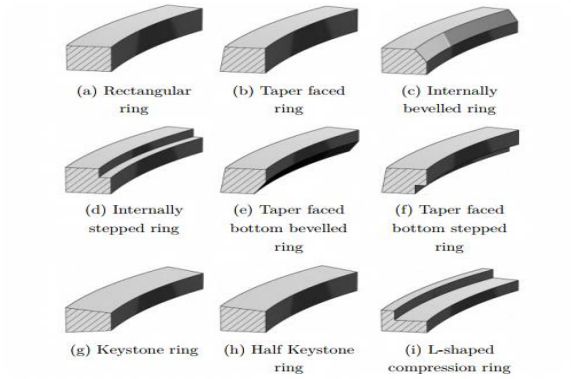

Figure 1.2 Compression ring cross sectional shape

II - LITERATURE REVIEW

The various researchers have been done research in the field of optimization of piston rings considering various parameters.

The piston rings are in charge of a substantial part of the fuel utilization in overwhelming obligation diesel motors. In this work Markus Soderfjalla et al (2017) utilized a fast segment test fix for assessment of piston ring contact. Various distinctive piston rings and barrel liners are assessed in view of their grating execution. Shear diminishing of run of the mill multi review oil is researched by contrasting it with single review oil.

Emil Wróblewski et al (2017) displayed the consequences of recreation for the ventured microgeometry piston bearing surface.*Sorin-Cristian Vlădescu et al (2017)* presents an exploratory examination into the stream conduct of grease in a responding contact reproducing a piston ring–chamber liner match. The point was to comprehend the impacts of cavitation, starvation and surface, and the association between these, so as to enhance car motor execution.

Reducing the fuel consumption of a combustion engine has been an important design issue. Engine friction has to be reduced and the piston ring - cylinder liner contact is a major source of friction. The *J. Fang et al (2016)* analyses the friction and load carrying capacity of an inclined parabolic at piston ring. This relatively simple geometry permits an analytical solution of the pressure distribution, the load carrying capacity and the friction. The friction coefficient is given as a function of twist angle, _at width and total width. The analytical expressions allow many thousands of calculations per second.

III-RESEARCH METHODOLOGY

3.1 Piston Ring Forces and Moments

The piston ring auxiliary movements can be isolated into piston ring movement the transverse way, piston ring turn, ring lift, and ring turn. These sorts of movement result from various burdens following up on the ring. Heaps of this kind are latency loads emerging from the piston speeding up and deceleration, oil film damping loads, loads attributable to the weight distinction over the ring, and rubbing loads from the sliding contact between the ring and barrel liner.

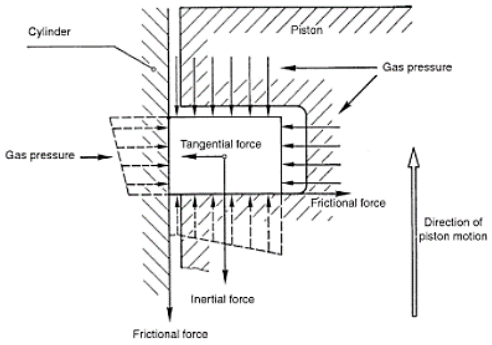

Figure 3.1 Forces acting on he Piston Ring (Handbook of Diesel Engines by Klaus Mollenhauer, Helmut Tschöke)

3.2 Piston Ring Relationships

The ring is squeezed against the barrel divider under a contact weight p which is represented by the measurements and aggregate free hole of the ring and by the modulus of flexibility of the material utilized. The aggregate free hole is characterized as the separation, measured along the impartial pivot, between the finishes of a piston ring in its uncompressed state.

Estimation of the contact pressure is tremendously challenging. Consequently, the solution is to calculate it from the tangential force. It can be defined as the force which when applied tangentially to the tops of the ring, is adequate to compress the ring to the quantified closed gap. By solving the

internal forces and moments, the following expressions are obtained (Bc. Jozef Dlugos)

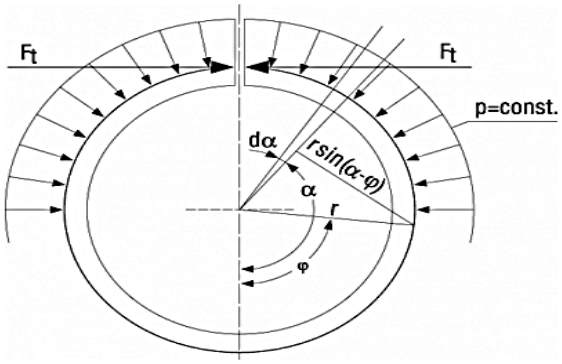

Figure 3.2 Forces applied on the piston ring surfaces.

$M = F_t r\,(1 + \cos\varphi)$ …… (1)

$M = phr^2\,(1 + \cos\varphi)$ …… (2)

where M is the bending moment and h is the axial width. By relating the bending moment of the constant contact pressure alongside of the tangential force, the subsequent relationship is recognized

$p = \frac{2F_t}{dh}$ …… (3)

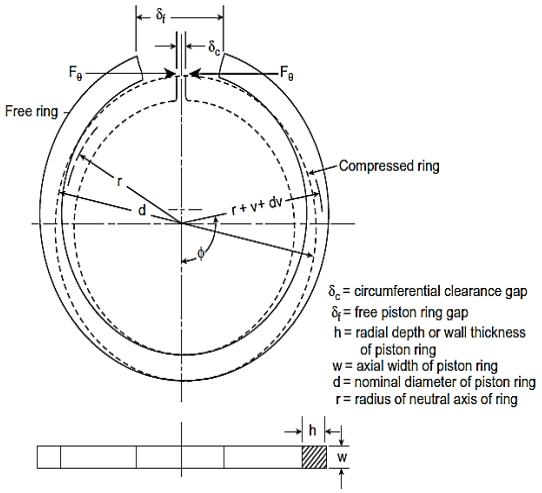

Figure3.3 Nomenclature of piston ring

3.2 Piston ring material

The piston ring materials need to meet extreme requests – quality at a high temperature, low unrelated power diminish because of temperature or weakness, consumption protection, great warm conductivity (for good warmth transferability to the barrel divider) and furthermore great sliding attributes for operation in typical and dry grease conditions - keeping in mind the end goal to withstand the warm and mechanical burdens during the running conditions.

3.3 Finite Element Analysis

3.3.1 General

The figure 3.4 shows the structure of phases to achieve a simulation. Many steps have taken during the analysis which are:

A. Part Definitions: - Created sketched
B. Material Descriptions: - Based on previous research done by various authors.
C. Boundary Conditions Explanations
D. Meshing
E. Solution and Simulation Controls
F. Post-processing
G. Restarting

Figure 3.4 Process for FEA analysis

3.3.2 Specification of the Problem

The objective of the present study is to examine the piston ring (compression ring) used in internal combustion engines with the three different material it is manufactured and for the comparison of two different cross section (Rectangular rings and Taper faced Rings). The solid model of the piston ring made in AutoCAD. Then model imported in ANSYS 14.0 for analysis.

3.3.3 Pre- processing

The Solid Modelling created using the AutoCAD and subsequently it is imported in ANSYS workbench.

3.3.3.1 Modeling of Piston Ring

The model dimension is a model of real time design of Piston ring used in IC engine as shown in figure 3.5. For the piston ring the outside radius R is 500 mm and minimal thickness is 2.2 mm as shown in figure 3.5. The CAD drawing is shown in figure 3.6.

Figure 3.5 (a)

Figure 3.5 (b)

Figure 3.5 (c)

Figure 3.5 (d)

Figure 3.5 (a,b,c and d) The actual Piston Ring considered for study.

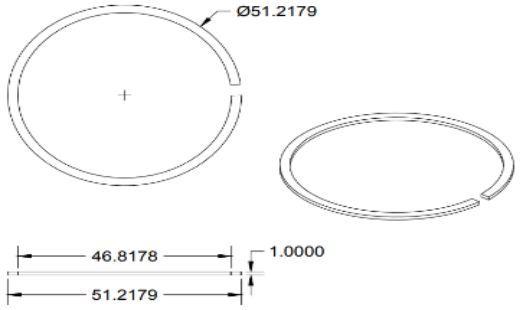

Figure 3.6 (a) Rectangular face Piston Ring layout

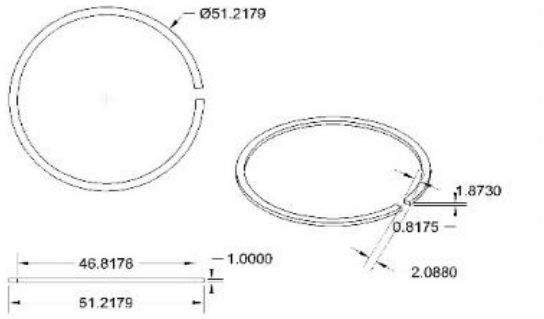

Figure 3.6 (b) Tapered face Piston Ring layout

3.3.3.2 Piston Ring Materials

There are three materials used for comparison

The Table 3.1 shows the material property for all different materials.

Table 3.3 Material properties

Property	Grey Cast Iron (Design Data Handbook)	Carbide malleable iron (Design Data Handbook)	Aluminium (K Satish Kumar)
Density	7.15	7.35	2.7
Hardness	208(Brinell)	250 (Brinell)	60 (Rockwell)
Tensile Strength ultimate (M Pa)	230-310	400-580	310
Yield Strength (M Pa)	460	483	280
Modulus of Elasticity (G Pa)	83-124	140-160	71

3.3.3 Discretization process (Meshing)

Structured meshing method done in ANSYS Workbench used for meshing the geometry. 3840 nodes and 441 elements created. The mesh model is presents in figure 3.4

Figure 3.7 Mesh model

3.4 Solutions

It is extremely hard to precisely show the cylinder ring, in which there are still inquiries about are going ahead to discover transient thermo flexible conduct of cylinder ring amid ignition process. There is dependably a need of a few suppositions to show any perplexing geometry. These suspicions are made, remembering the challenges associated with the hypothetical computation and the significance of the parameters that are taken and those which are disregarded. In displaying we generally overlook the things that are of less significance and have little effect on the examination. The suppositions are constantly made relying on the subtle elements and precision required in demonstrating. The Boundary conditions applied is shown in figure 3.8

The finite element analysis carried out on the three-different material pressure ring. In the following the boundary conditions and assumptions applied are as:

1. The piston ring material is assumed as homogeneous and isotropic.
2. Inertia and body constrain impacts are unimportant amid the examination.
3. The piston ring is well-thought-out stress free earlier the analysis.
4. The examination does not decide the life of the compression ring.
5. Only ambient air-cooling considered without the forced Convection.
6. Uniform thermal conductivity of the
7. Constant specific heat of the material
8. Minimum wall pressure for piston rings of IC engines is considered as 0.059 MPa (Design data hand book)
9. The Bulk temperature is considered as 22°C

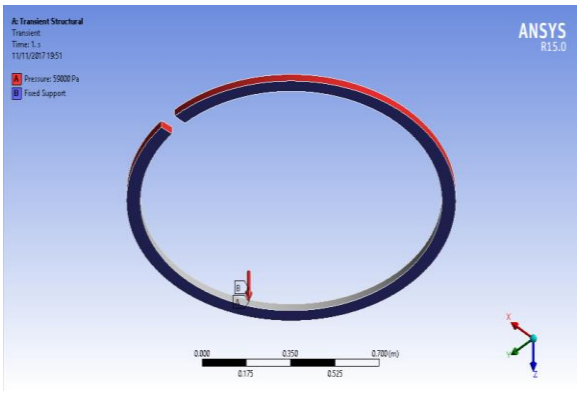

Figure 3.8 (a) Structural Boundary Conditions applied for the study

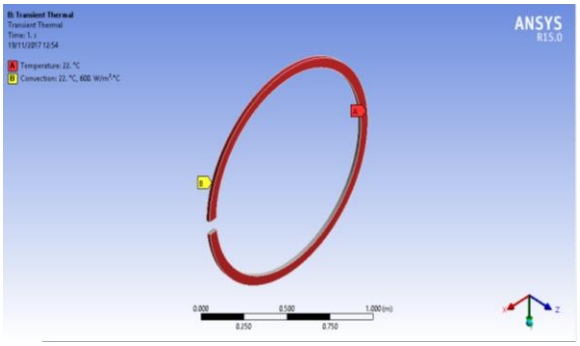

Figure 3.8 (b) Thermal Boundary Conditions applied for the study

IV -RESULT ANALYSIS

The chapter contains the FE results obtained from analysis. There are two different piston rings with three different materials are considered for analysis.

4.1 Piston Rings of Rectangular Cross Section

Figure 4.1 to 4.32 shows the results regarding total deformation, Directional Deformation, Elastic Strain, Von-Mises Stress, Maximum Shear Stress Strain Energy, Total Heat Flux and Directional Heat Flux distribution respectively for Grey cast Iron, Aluminium Alloy and Carbide Malleable Iron material.

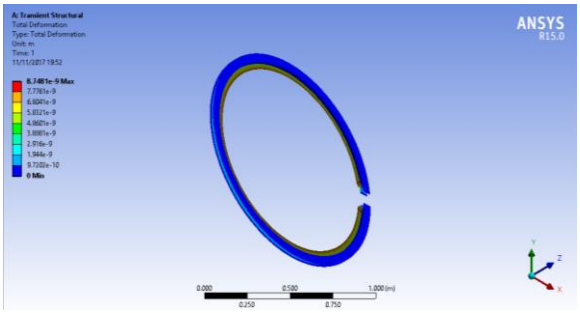

Figure 4.1 Total Deformation in Rectangular Piston Ring of Grey Cast Iron

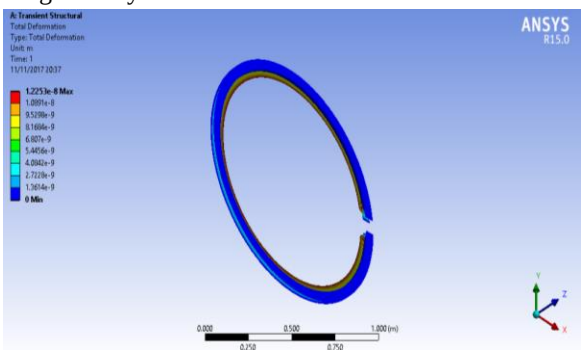

Figure 4.2 Total Deformation in Rectangular Piston Ring of Aluminium Alloy material

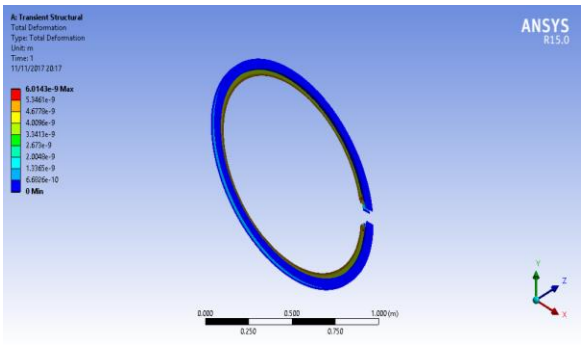

Figure 4.3 Total Deformation in Rectangular Piston Ring of Carbide Malleable Iron material

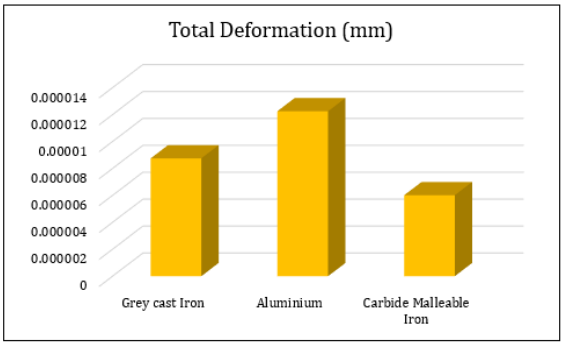

Figure 4.4 Comparison of Total Deformation for All the Three Material Rectangular Piston Ring

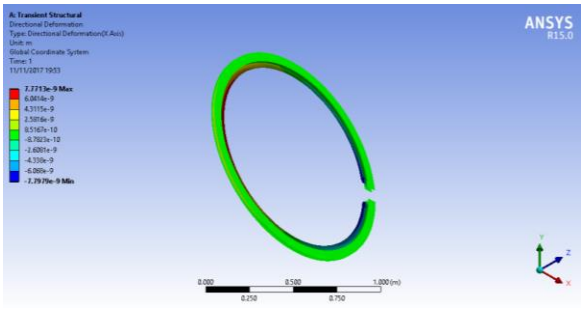

Figure 4.5 Directional Deformation in Rectangular Piston Ring of Grey Cast Iron

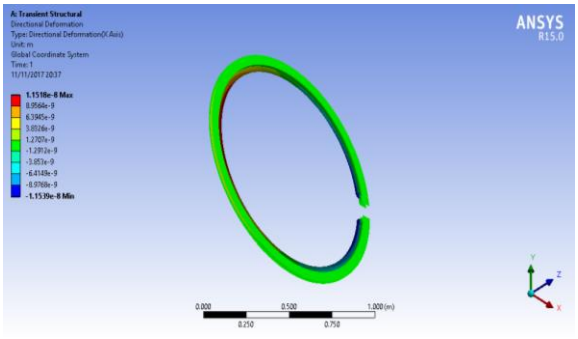

Figure 4.6 Directional Deformation in Rectangular Piston Ring of Aluminium Material

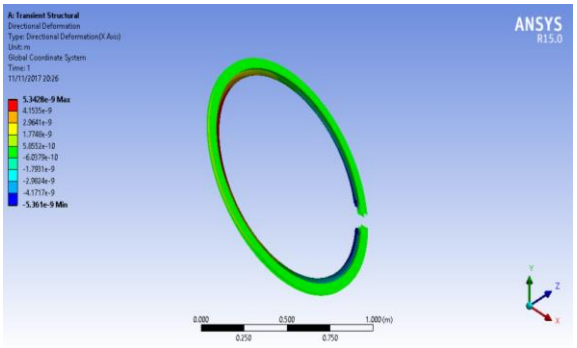

Figure 4.7 Directional Deformation in Rectangular Piston Ring of Carbide Malleable Iron Material

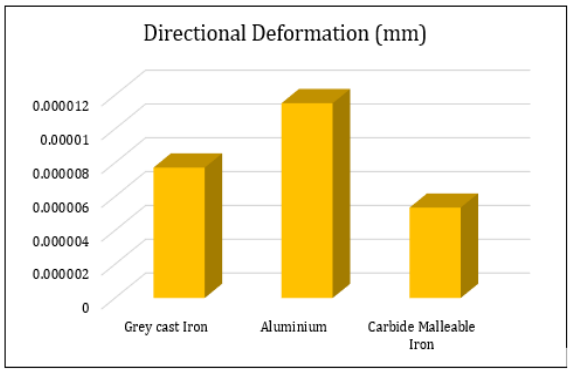

Figure 4.8 Comparison of Directional Deformation for All the Three Material Rectangular Piston Ring

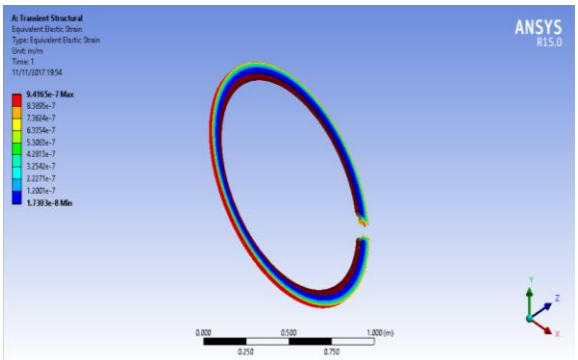

Figure 4.9 Von Mises Strain in Rectangular Piston Ring of Grey Cast Iron

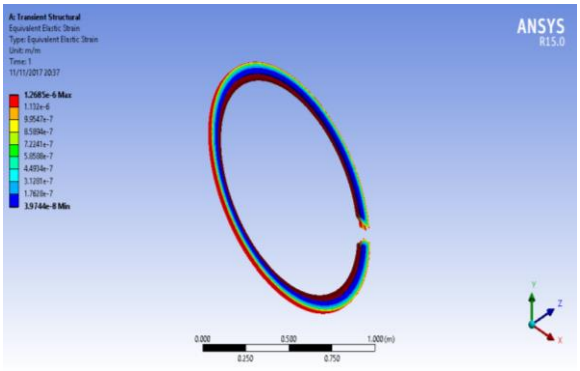

Figure 4.10 Von Mises Strain in Rectangular Piston Ring of Aluminium Alloy Material

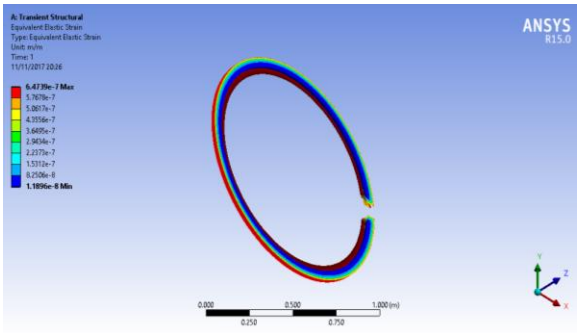

Figure 4.11 Von Mises Strain in Rectangular Piston Ring of Carbide Malleable Iron Material

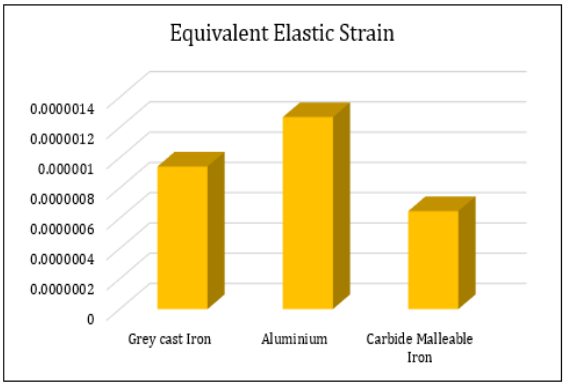

Figure 4.12 Comparison of Equivalent Elastic Strain for All the Three Material Rectangular Piston Ring

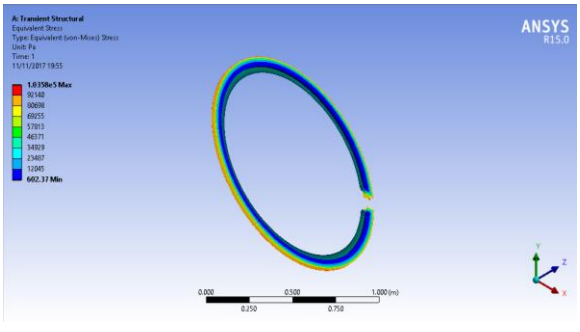

Figure 4.13 Von-Mises Stress in Rectangular Piston Ring of Grey Cast Iron

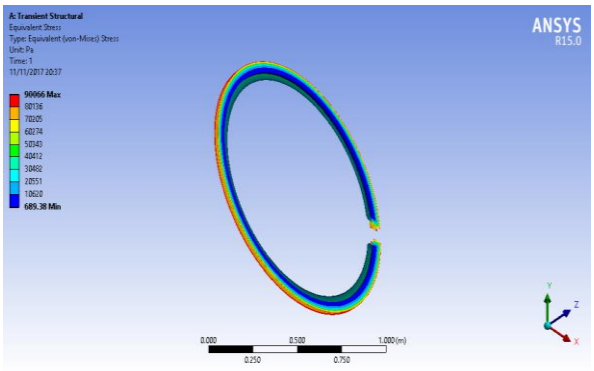

Figure 4.14 Von-Mises Stress in Rectangular Piston Ring of aluminium Alloy Material

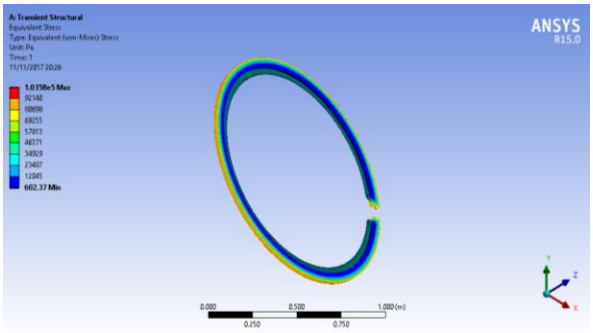

Figure 4.15 Von-Mises Stress in Rectangular Piston Ring of Carbide Malleable Iron Material

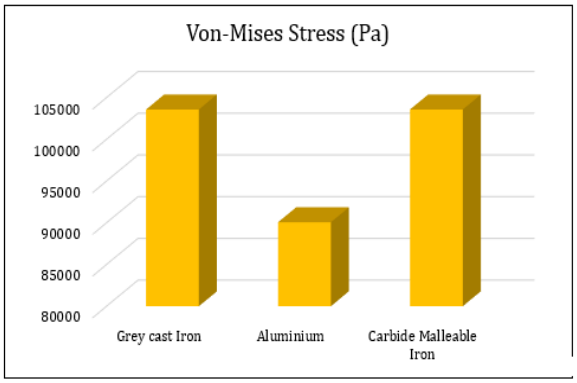

Figure 4.16 Comparison of Equivalent Elastic Stress for All the Three Material Rectangular Piston Ring

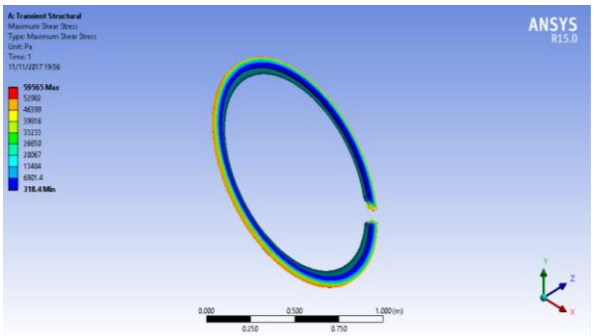

Figure 4.17 Maximum Shear Stress in Rectangular Piston Ring of Grey Cast Iron

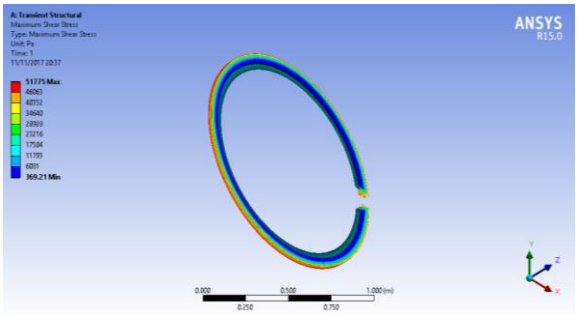

Figure 4.18 Maximum Shear Stress in Rectangular Piston Ring of Aluminium Alloy Material

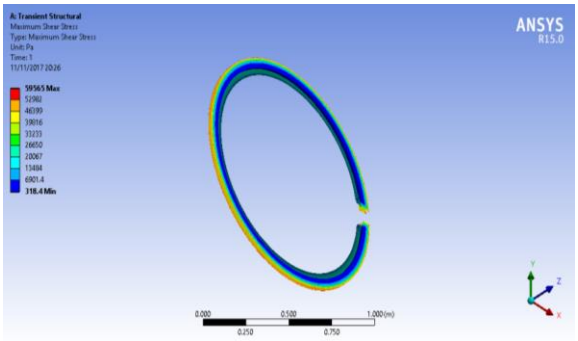

Figure 4.19 Maximum Shear Stress in Rectangular Piston Ring of Carbide Malleable Iron Material

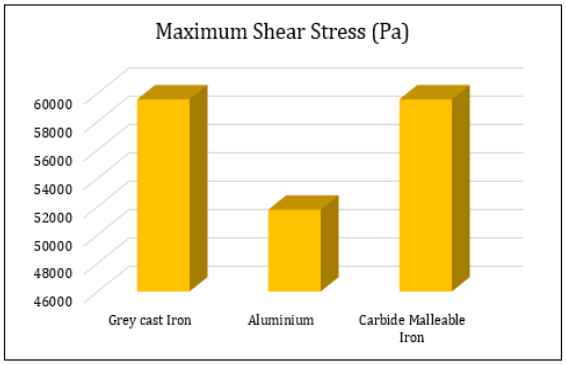

Figure 4.20 Comparison of Maximum Shear Stress for All the Three Material Rectangular Piston Ring

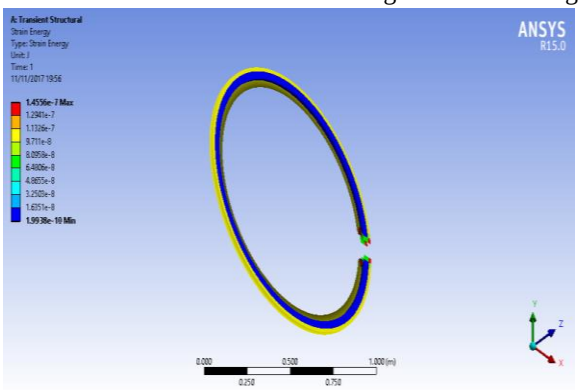

Figure 4.21 Strain Energy in Rectangular Piston Ring of Grey Cast Iron

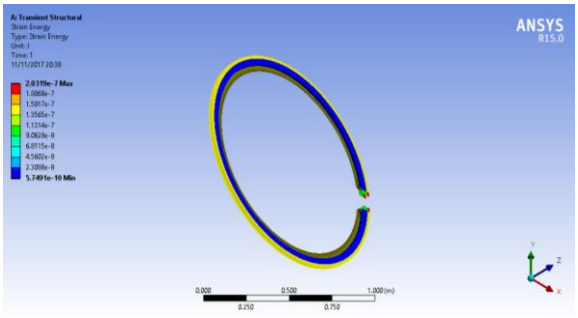

Figure 4.22 Strain Energy in Rectangular Piston Ring of Aluminium Alloy Material

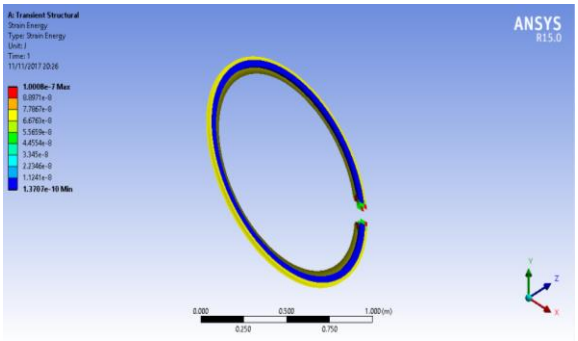

Figure 4.23 Strain Energy in Rectangular Piston Ring of Carbide Malleable Iron Material

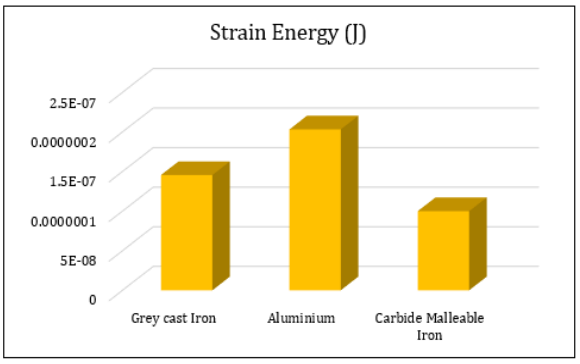

Figure 4.24 Comparison of Strain Energy for All the Three Material Rectangular Piston Ring

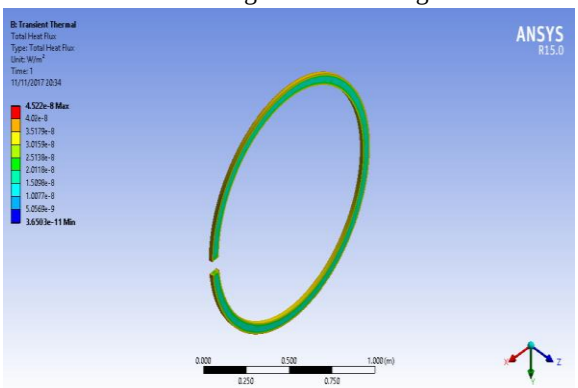

Figure 4.25 Total Heat Flux in Rectangular Piston Ring of Grey Cast Iron

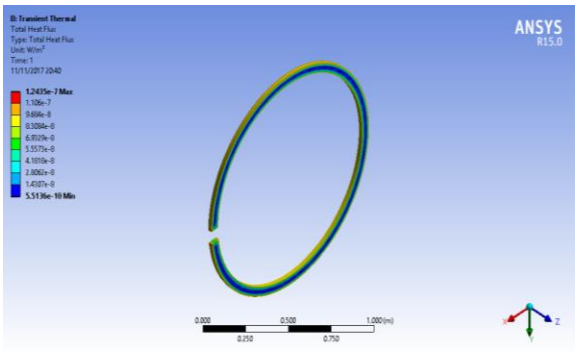

Figure 4.26 Total Heat Flux in Rectangular Piston Ring of Aluminium Alloy Material

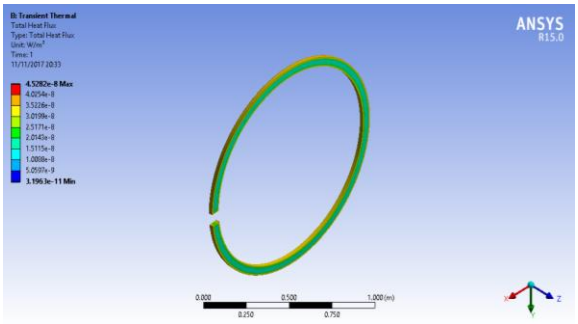

Figure 4.27 Total Heat Flux in Rectangular Piston Ring of Carbide Malleable Iron Material

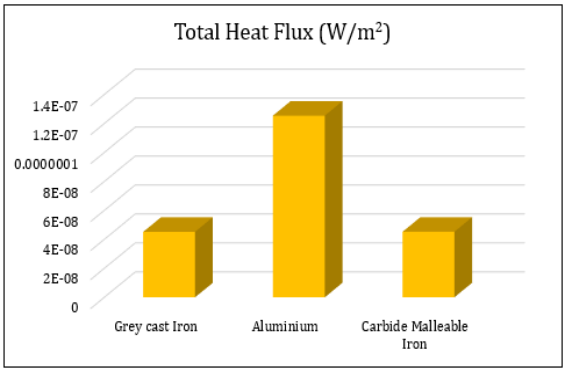

Figure 4.28 Comparison of Total Heat Flux for All the Three Material Rectangular Piston Ring

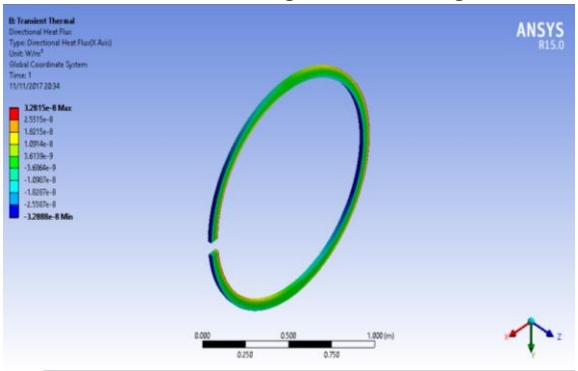

Figure 4.29 Directional Heat Flux in Rectangular Piston Ring of Grey Cast Iron

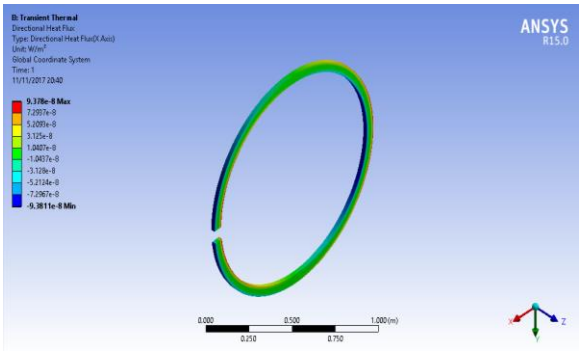

Figure 4.30 Directional Heat Flux in Rectangular Piston Ring of Aluminium Alloy Material

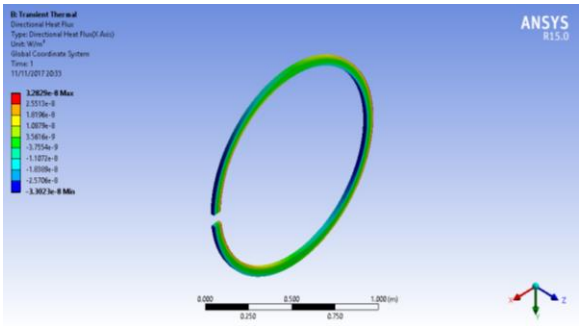

Figure 4.31 Directional Heat Flux in Rectangular Piston Ring of Carbide Malleable Iron Material

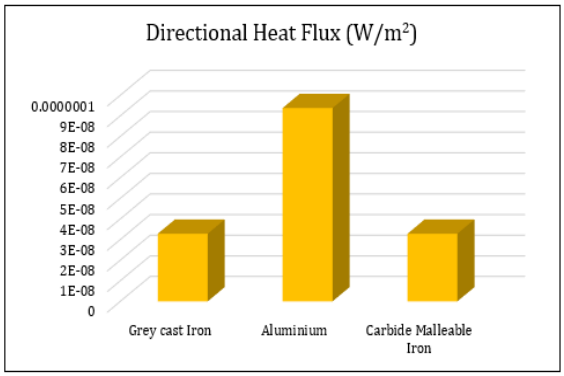

Figure 4.32 Comparison of Total Heat Flux for All the Three Material Rectangular Piston Ring

4.2 Piston Rings of Taper Faced Cross Section

Figure 4.33 to 4.60 shows the results regarding total deformation, Directional Deformation, Elastic Strain, Von-Mises Stress, Maximum Shear Stress Strain Energy, Total Heat Flux and Directional Heat Flux distribution respectively for Grey cast Iron, Aluminium Alloy and Carbide Malleable Iron material.

Figure 4.33 to 4.35 shows the Total Deformation in mm for all the three materials piston ring.

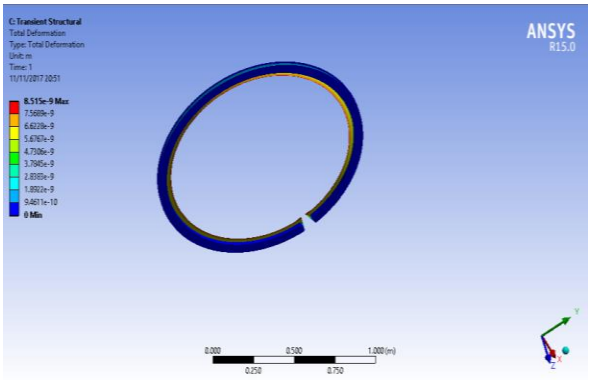

Figure 4.33 Total Deformation in Taper Faced Piston Ring of Grey Cast Iron Material

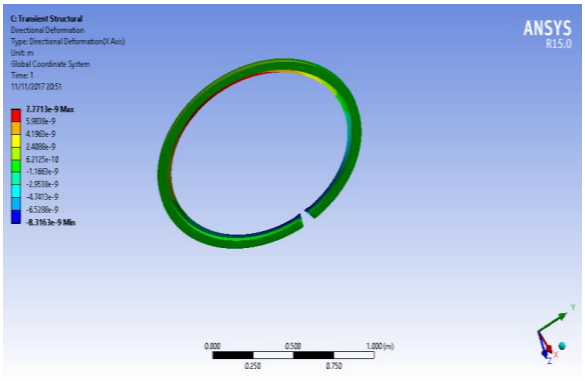

Figure 4.37 Directional Deformation in Taper Faced Piston Ring of Grey Cast Iron Material

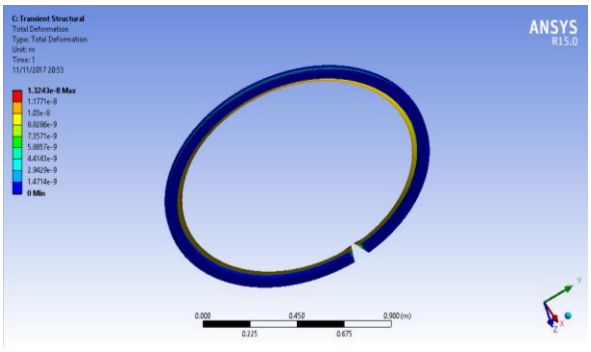

Figure 4.34 Total Deformation in Taper Faced Piston Ring of Aluminium Alloy Material

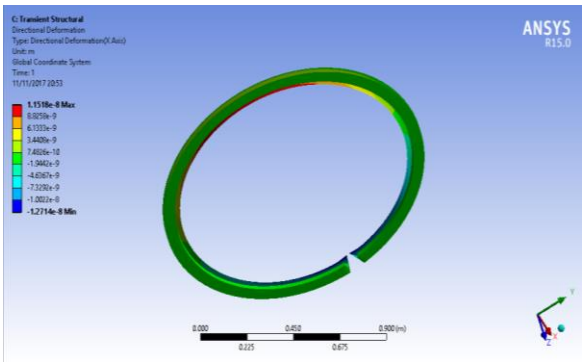

Figure 4.38 Directional Deformation in Taper Faced Piston Ring of Aluminium Alloy Material

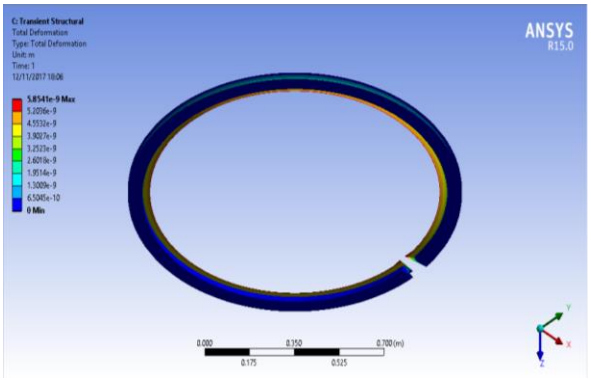

Figure 4.35 Total Deformation in Taper Faced Piston Ring of Carbide Malleable Iron Material

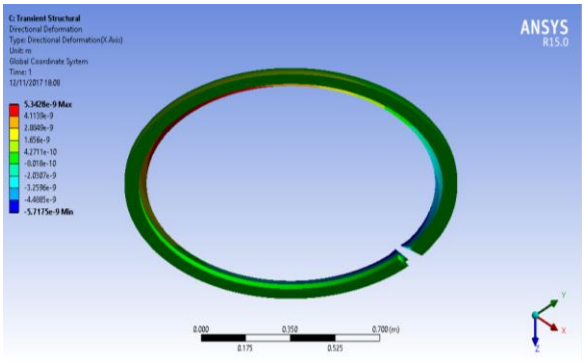

Figure 4.39 Directional Deformation in Taper Faced Piston Ring of Carbide Malleable Iron Material

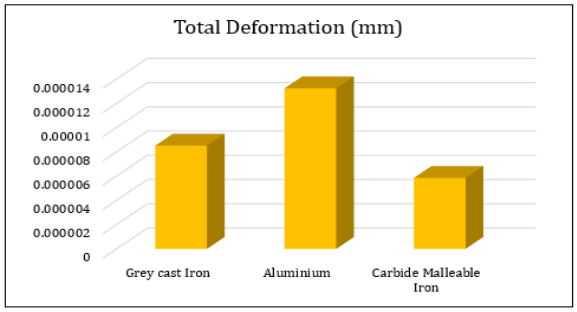

Figure 4.36 Comparison of Total Deformation for All the Three Material Tapered Face Piston Ring

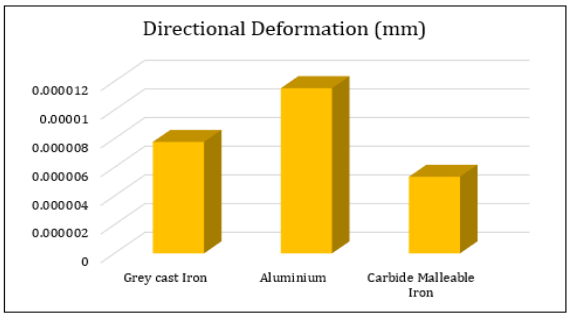

Figure 4.40 Comparison of Directional Deformation for All the Three Material Tapered Face Piston Ring

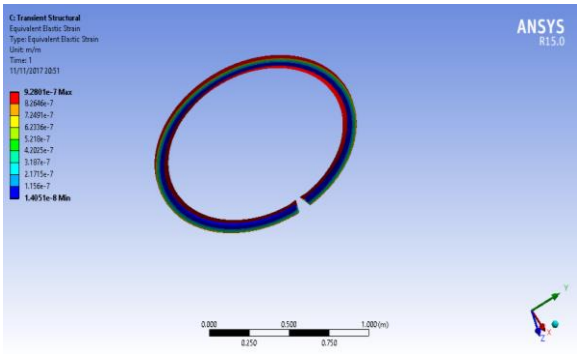

Figure 4.41 Von Mises Strain in Taper Faced Piston Ring of Grey Cast Iron Material

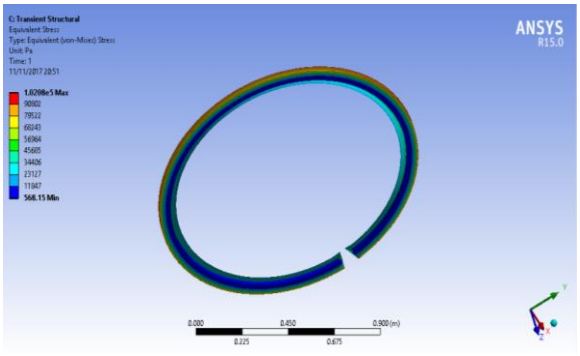

Figure 4.45 Von Mises Stress in Taper Faced Piston Ring of Grey Cast Iron Material

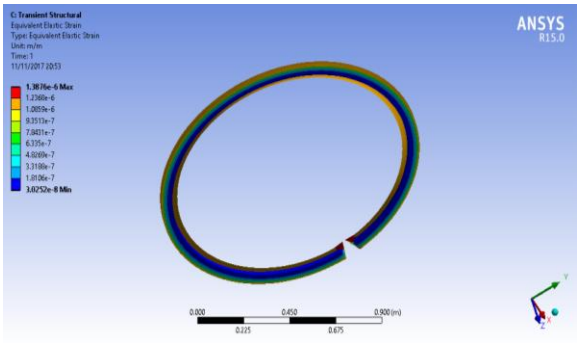

Figure 4.42 Von Mises Strain in Taper Faced Piston Ring of Aluminium Alloy Material

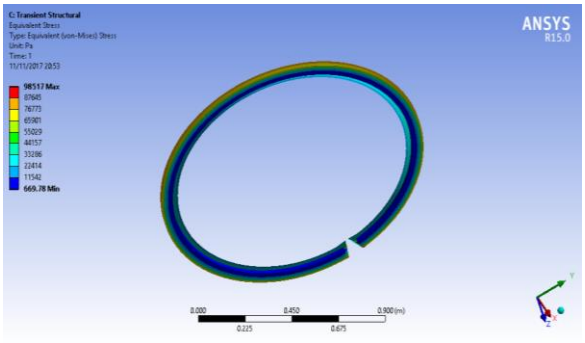

Figure 4.46 Von Mises Stress in Taper Faced Piston Ring of Aluminium Alloy Material

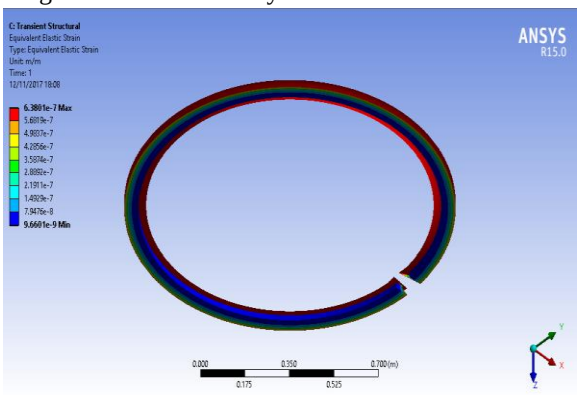

Figure 4.43 Von Mises Strain in Taper Faced Piston Ring of Carbide Malleable Iron Material

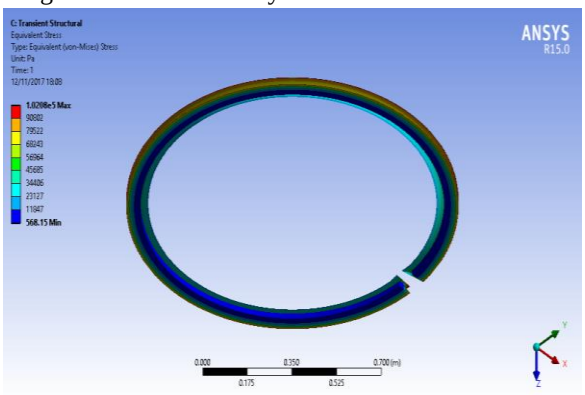

Figure 4.47 Von Mises Stress in Taper Faced Piston Ring of Carbide Malleable Iron Material

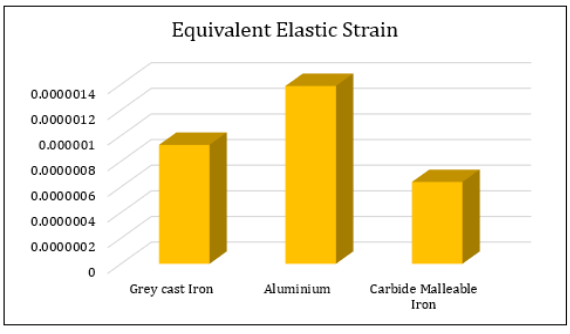

Figure 4.44 Comparison of Equivalent Elastic Strain for All the Three Material Tapered Face Piston Ring

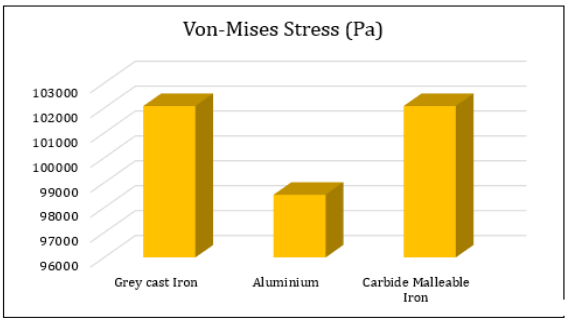

Figure 4.48 Comparison of Von-Mises Stress for All the Three Material Tapered Face Piston Ring

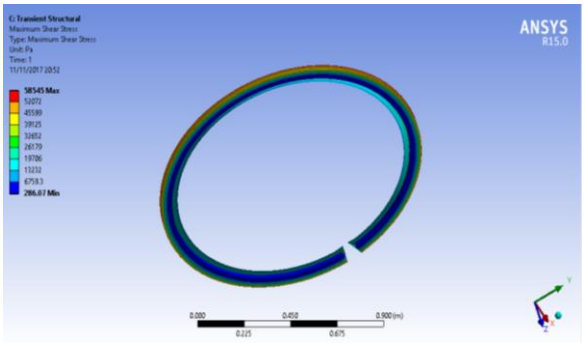

Figure 4.49 Maximum Shear Stress in Taper Faced Piston Ring of Grey Cast Iron Material

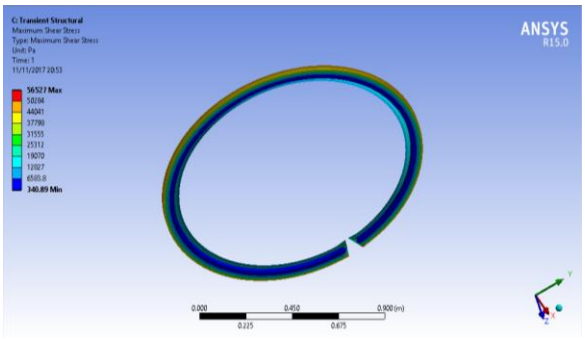

Figure 4.50 Maximum Shear Stress in Taper Faced Piston Ring of Aluminium Alloy Material

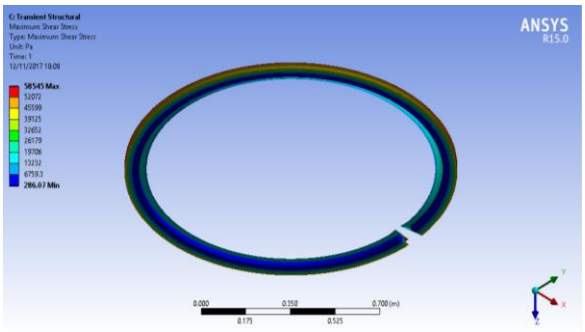

Figure 4.51 Maximum Shear Stress in Taper Faced Piston Ring of Carbide Malleable Iron Material

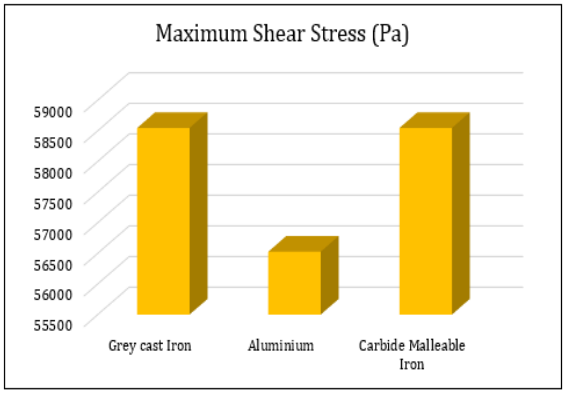

Figure 4.52 Comparison of Maximum Shear Stress for All the Three Material Tapered Face Piston Ring

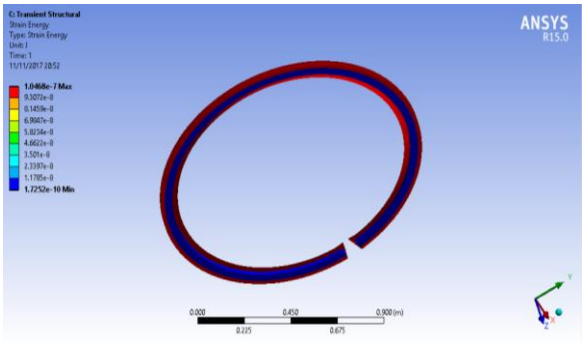

Figure 4.53 Strain energy in Taper Faced Piston Ring of Grey Cast Iron Material

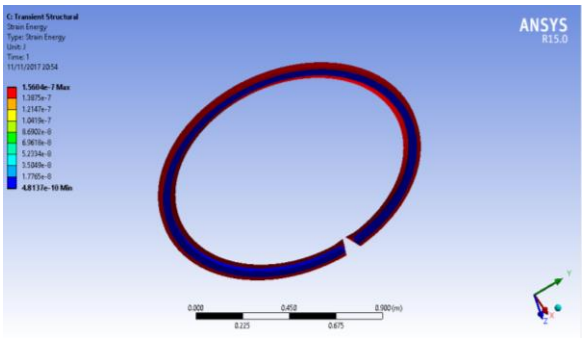

Figure 4.54 Strain energy in Taper Faced Piston Ring of Aluminium Alloy Material

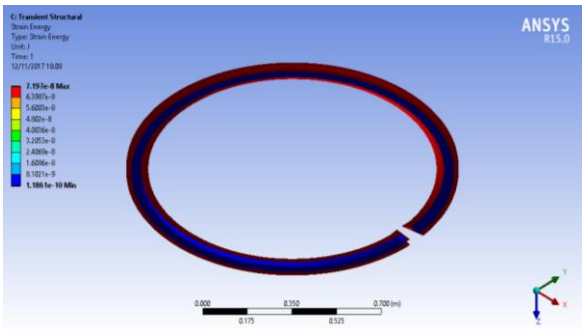

Figure 4.55 Strain energy in Taper Faced Piston Ring of Carbide Malleable Iron Material

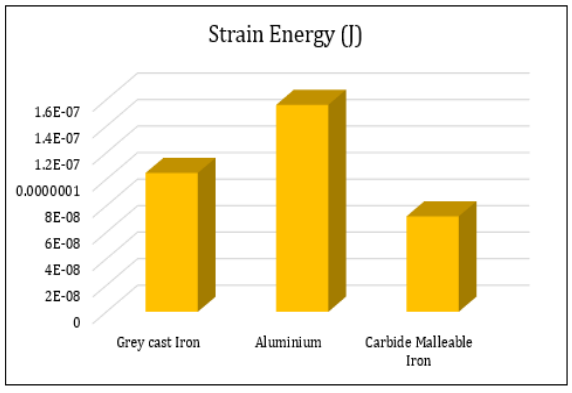

Figure 4.56 Comparison of Strain Energy for All the Three Material Tapered Face Piston Ring

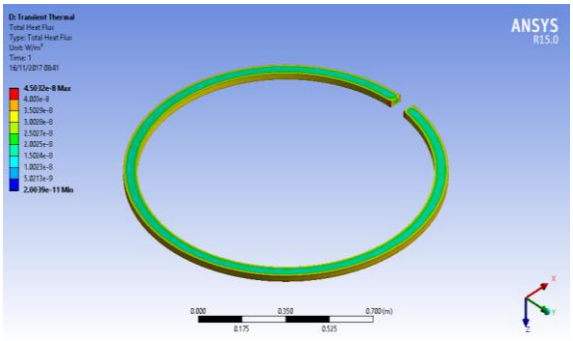

Figure 4.57 Total Heat Flux in Taper Faced Piston Ring of Grey cast Iron Material

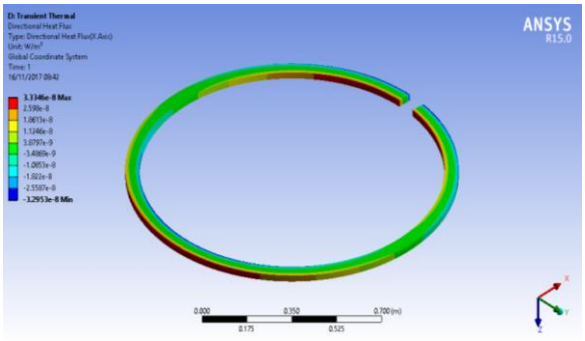

Figure 4.61 Directional Heat Flux in Taper Faced Piston Ring of Grey Cast Iron Material

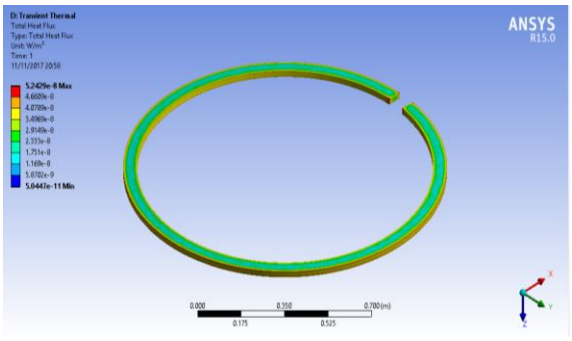

Figure 4.58 Total Heat Flux in Taper Faced Piston Ring of Aluminium Alloy Material

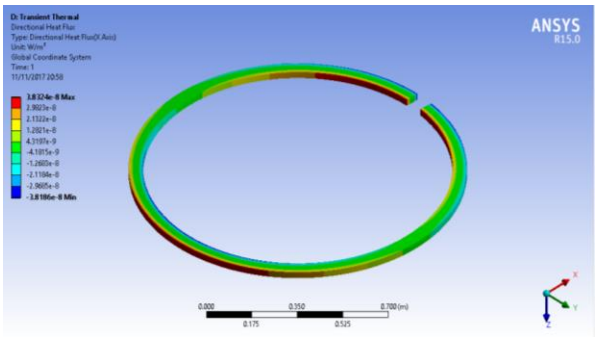

Figure 4.62 Directional Heat Flux in Taper Faced Piston Ring of Aluminium Alloy Material

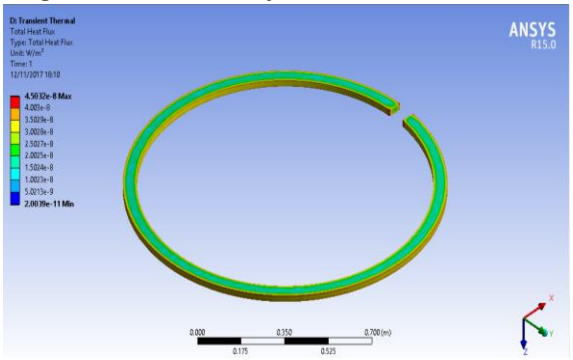

Figure 4.59 Total Heat Flux in Taper Faced Piston Ring of Carbide Malleable Iron Material

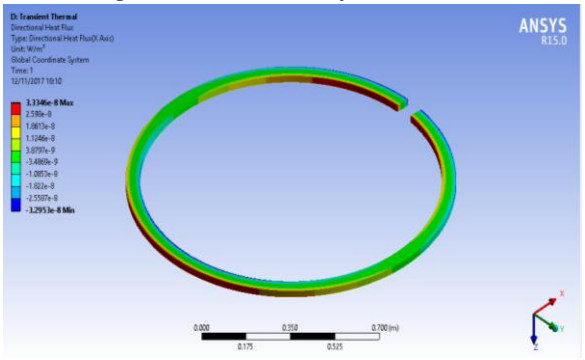

Figure 4.63 Directional Heat Flux in Taper Faced Piston Ring of Carbide Malleable Iron Material

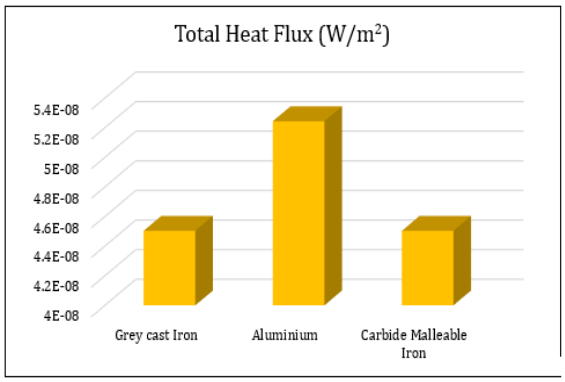

Figure 4.60 Comparison of Total Heat Flux for All the Three Material Tapered Face Piston Ring

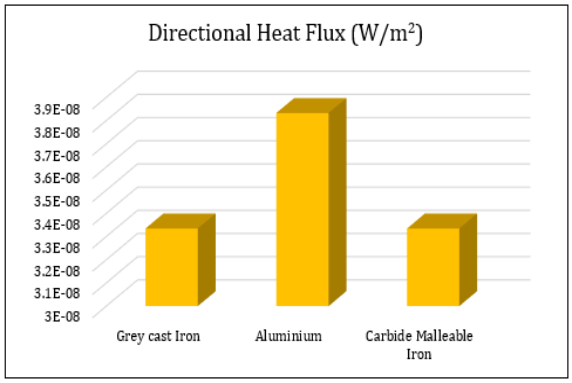

Figure 4.60 Comparison of Directional Heat Flux for All the Three Material Tapered Face Piston Ring

Table 4.1 Summarized results for Rectangular Cross Section Piston Ring

Parameter	Grey cast Iron	Aluminum	Carbide Malleable Iron
Total Deformation (mm)	0.000008748	0.00001225	6.0143×10^{-06}
Directional Deformation (mm)	0.00000771	0.000011518	5.3428×10^{-06}
Equivalent Elastic Strain	9.416×10^{-07}	0.000001268	6.4739×10^{-07}
Von-Mises Stress (Pa)	103580	90066	10358
Maximum Shear Stress (Pa)	59565	51775	59565
Strain Energy (J)	1.4556×10^{-07}	2.0319×10^{-07}	1.00008×10^{-07}
Total Heat Flux (W/m2)	4.522×10^{-08}	1.2543×10^{-07}	4.5282×10^{-08}
Directional Heat Flux (W/m²)	3.2815×10^{-08}	9.378×10^{-08}	3.2829×10^{-08}

Table 4.2 Summarized results for Taper Faced Cross Section Piston Ring

Parameter	Grey cast Iron	Aluminium	Carbide Malleable Iron
Total Deformation (mm)	0.000008515	0.000013243	5.8541×10^{-06}
Directional Deformation (mm)	7.7713×10^{-06}	0.000011518	5.3428×10^{-06}
Equivalent Elastic Strain	9.2801×10^{-07}	1.3876×10^{-06}	6.3801×10^{-07}
Von-Mises Stress (Pa)	102080	98517	102080
Maximum Shear Stress (Pa)	58545	56527	58545
Strain Energy (J)	1.0468×10^{-07}	1.5604×10^{-07}	7.197×10^{-08}
Total Heat Flux (W/m²)	4.5032×10^{-08}	5.2429×10^{-08}	4.5032×10^{-08}
Directional Heat Flux (W/m²)	3.3346×10^{-08}	3.8324×10^{-08}	3.3346×10^{-08}

V-CONCLUSION

In this work finite element analysis for static and dynamic conditions of the engine piston ring of different cross section with different materials was performed. The following conclusion has been made after the study.

The Total Deformation is about 8.748×10^{-6} mm for Grey Cast Iron, 1.225×10^{-5} mm for Aluminium alloy and 6.0145×10^{-6} mm for Carbide Malleable Iron in case of Rectangular cross section piston ring while it is about 8.515×10^{-6} mm for Grey Cast Iron, 1.3243×10^{-5} mm for Aluminium alloy and 5.8541×10^{-6} mm for Carbide Malleable Iron in case of Tapered face piston ring.

The Aluminium material piston ring shows the more elastic strain compare then other two in both type of piston rings. Carbide Malleable Iron piston ring shows the less elastic strain in both type of piston rings. But if compare the individual material piston ring of same material the tapered face piston rings of Grey Cast Iron and Carbide Malleable Cast Iron shows the less elastic strain compare then rectangular cross section piston rings. The condition is opposite when we consider aluminium alloy rings.

The maximum and minimum value Von-Mises stress or equivalent Stress for all three materials piston rings with both cross sections are in safe limit.

The value of Shear stress for all three materials piston rings with both cross sections are in safe limit. Thus it can be stated that the design is safe from shear stress point of view. The tapered face piston rings of Grey Cast Iron and Carbide Malleable Cast Iron shows the less shear stress compare then rectangular cross section piston rings while it is more in rectangular cross section rings aluminium alloy rings.

Aluminium shows the maximum strain energy while Carbide malleable piston ring shows the minimum strain energy.

Aluminium alloy piston ring shows the High Total heat flux and directional heat while Both of Iron material piston ring shows the same but lower Total and directional heat flux in case of both Rectangular cross section piston rings and Tapered face piston rings. In rectangular face piston rings of Grey cast Iron and Carbide Malleable Iron less heat flux is generated which can be the prime factor of best suitability, while aluminium alloy rectangular piston rings generates high heat flux.

REFERENCES

[1] Bc. JOZEF Dlugos 2014, "Computational Modelling Of Piston Ring Dynamics", Brno University of Technology.

[2] C. Kirner, J. Halbhuber, B. Uhlig, A. Oliva, S. Graf and G. Wachtmeister, 2016 "Experimental and simulative research advances in the piston assembly of an internal combustion engine," Tribiology International

[3] C. Pettavino, N. Biboulet and A.A. Lubrecht, Load carrying capacity and friction of a parabolic-flat piston ring of finite width, Tribiology International

[4] Chittenden R. J. and Priest M. Analysis of the piston assembly, bore distortion and future developments. In: Taylor, C.M. (Ed.). Engine Tribology. Elsevier, 1993, Tribology series, 26, pp. 241–270. ISBN 0-444-89755-0.

[5] Dowson, D. Piston assemblies; background and lubrication analysis. In: Taylor, C.M. (ed.). Engine Tribology. Elsevier, 1993, Tribology series, 26, pp. 213–240. ISBN 0-444-89755-0.

[6] Emil Wróblewski, Antoni Iskraa, Maciej Babiaka, 2017, "Geometrical structures of the stepped profile bearing surface of the piston", TRANSCOM 2017: International scientific conference on sustainable, modern and safe transport.

[7] Isam Jasim Jaber and Ajeet Kumar Rai, 2014, "Design and Analysis of I.C. Engine Piston and Piston-Ring Using Catia and Ansys Software", International Journal of Mechanical Engineering and Technology (IJMET), ISSN 0976 – 6340(Print), ISSN 0976 – 6359(Online), Volume 5, Issue 2, February (2014), pp. 64-73, © IAEME

[8] J. Fang, W. Ma, N. Biboulet and A.A. Lubrecht, "Load carrying capacity and friction of an inclined parabolic-flat piston ring", Tribiology International

[9] Jianliang Lin, RonghuaWei, Daniel Christopher Bitsis, Peter M. Lee, 2016, "Development and evaluation of low friction TiSiCN nano-composite coatings for piston ring applications", Surface & Coatings Technology 298 (2016) 121–131

[10] K. Sathish Kumar, 2016, "Design and Analysis of I.C. Engine Piston and Piston-Ring on Composite Material Using Creo and Ansys Software", Journal of Engineering and Science Vol. 01, Special Issue 01, July 2016

[11] Krisada Wannatong, Somchai Chanchaona, Surachai Sanitjai, 2008, "Simulation algorithm for piston ring dynamics", Simulation Modelling Practice and Theory 16 (2008) 127–146

[12] Markus Söderfjäll, Andreas Almqvist, Roland Larsson, 2016, "Component test for simulation of piston ring – Cylinder liner friction at realistic speeds", Tribology International 104(2016)57–63

[13] Markus Sooderfjall, Hubert M. Herbst , Roland Larsson , Andreas Almqvist , 2017, "Influence on friction from piston ring design, cylinder liner roughness and lubricant properties", Tribology International 116 (2017) 272–284

[14] N. Biboulet, A.A.Lubrecht, 2016, "Analytical solution for textured piston ring – Cylinder liner contacts (1D analysis)", Tribology International 96(2016)269–278.

[15] O. Carvalho , M. Buciumeanu ,S. Madeira, D. Soares , F.S. Silva , G. Miranda, 2015, "Optimization of AlSi–CNTs functionally graded material composites for engine piston rings", Materials and Design 80 (2015) 163–173

[16] Pavlo Lyubarskyy and Dirk Bartel, 2D CFD-Model of the Piston Assembly in a Diesel Engine for the Analysis of Piston Ring Dynamics, Mass Transport and Friction, Tribiology International

[17] Parthiban S, Arshad Mohamed Gani P, Vasudevan R, Naveen Kumar C, 2015, " Design and Performance Analysis on Piston Ring" International Journal of Engineering Research and General Science Volume 3, Issue 5, September-October, 2015 ISSN 2091-2730

[18] Röhrle, M. D. Pistons for internal combustion engines – fundamentals of piston technology, MAHLE GmbH. Verlag Moderne Industry. Landsberg/Lech, Germany. 1995. p. 70.

[19] Sorin-Cristian Vlădescua, Alessandra Cinieroa, Khizer Tufail, Arup Gangopadhyay, Tom Reddyhoff, 2017, "Looking into a laser textured piston ring-liner contact", Tribology International 115 (2017) 140–153

[20] T Tian, 2001, "Dynamic behaviors of piston rings and their practical impact. Part 2: oil transport, friction and wear of ring/ liner interface and the effects of piston and ring dynamics", Proc Instn Mech Engrs Vol 216 Downloaded from pij.sagepub.com at COLUMBIA UNIV on February 5, 2015 Part J: J Engineering Tribology

[21] Xingsong Wang, Xiaosong Chen, 2010, "Measuring radial pressure distributions of piston rings based on partial-thin-walled cylinder", Measurement 43 (2010) 197–203